Asymmetric, helical and mirror-symmetric travelling waves in pipe flow

Chris Pringle* and Rich R. Kerswell†
Department of Mathematics, University of Bristol,
University Walk, Bristol BS8 1TW, United Kingdom
(Dated: March 26, 2007)

New families of three-dimensional nonlinear travelling waves are discovered in pipe flow. In contrast to known waves (Faisst & Eckhardt *Phys. Rev. Lett.* **91**, 224502 (2003), Wedin & Kerswell, *J. Fluid Mech.* **508**, 333 (2004)), they possess no rotational symmetry and exist at much lower Reynolds numbers. Particularly striking is an 'asymmetric mode' which has one slow streak sandwiched between two fast streaks located preferentially to one side of the pipe. This family originates in a pitchfork bifurcation from a mirror-symmetric travelling wave which can be traced down to a Reynolds number of 773. Helical and non-helical rotating waves are also found emphasizing the richness of phase space even at these very low Reynolds numbers. The delay in Reynolds number from when the laminar state ceases to be a global attractor to turbulent transition is then even larger than previously thought.

PACS numbers: 47.20.Ft,47.27.Cn,47.27.nf

Wall-bounded shear flows are of tremendous practical importance yet their transition to turbulence is still poorly understood. The oldest and most famous example is the stability of flow along a straight pipe of circular cross-section first studied over 120 years ago [1]. A steady, unidirectional, laminar solution - Hagen-Poiseuille flow [2, 3] - always exists but is only realised experimentally for lower flow rates (measured by the Reynolds number $Re = UD/\nu$, where U is the mean axial flow speed, D is the pipe diameter and ν is the fluid's kinematic viscosity). At higher Re, the fluid selects a state which is immediately spatially and temporally complex rather than adopting a sequence of intermediate states of gradually decreasing symmetry. The exact transition Reynolds number Re_t depends sensitively on the shape and amplitude of the disturbance present and therefore varies across experiments with quoted values typically ranging from 2300 down to a more recent estimate of 1750 ([4, 5, 6, 7, 8, 9, 10, 11, 12]). A new direction in rationalising this abrupt transition revolves around identifying alternative solutions (beyond the laminar state) to the governing Navier-Stokes equations. These have only recently be found in the form of travelling waves (TWs) [13, 14] and all seem to be saddle points in phase space. They appear though saddle node bifurcations with the lowest found at $Re = 1251$. The delay before transition occurs ($Re_t \geq 1750$) is attributed to the need for phase space to become sufficiently complicated (through the entanglement of stable and unstable manifolds of an increasing number of saddle points) to support turbulent trajectories.

In this Letter, we present four new families of 'asymmetric', 'mirror-symmetric', helical and non-helical rotating TWs which have different structure to known solutions and exist at lower Reynolds numbers. The asymmetric family, which have one slow streak sandwiched between two fast streaks located preferentially to one side of the pipe, are particularly significant as they are the missing family of rotationally-asymmetric waves not found in [13, 14] and have the structure preferred by the linear transient growth mechanism [15]. They bifurcate from a new mirror-symmetric family which can be traced down to a saddle node bifurcation at $Re = 773$. This figure substantially lowers the current best estimate of 1251 for Re_g - the Reynolds number at which the laminar state stops being a global attractor. The relative sizes of this new Re_g and Re_t for pipe flow are then more in line with plane Couette flow ($Re_t = 323$ [16] and $Re_g = 127.7$ [17, 18]: Re based on half the velocity difference and half the channel width) than plane Poiseuille flow ($Re_t \approx 1300$ [19, 20, 21, 22, 23] and $Re_g = 860$ [18]: Re based on the mean flow rate and the channel width). Beyond suggesting that Re_g in plane Poiseuille flow can be significantly lowered, these latest discoveries highlight the substantial delay in Re between new solutions appearing in phase space and the emergence of sustained turbulent trajectories.

The new solutions were captured by inserting a fully 3-dimensional spectral representation (Chebychev in s, Fourier in ϕ and z where (s, ϕ, z) are the usual cylindrical coordinates aligned with the pipe) of the velocity and pressure field into the governing Navier-Stokes equations as viewed from an appropriately rotating and translating reference frame in which the TW is steady [14]. The resultant nonlinear algebraic system was solved using the Newton-Raphson algorithm [30]. To start the procedure off, an artificial body force was added to the Navier-Stokes equations (see [14]) designed to give streamwise-independent vortices and streaks of a finite amplitude. The size of the forcing was then adjusted to find a bifurcation point at which the translational flow symmetry along the pipe is broken. New finite-amplitude solutions to pipe flow were found if this solution branch could be continued back to the zero-forcing limit.

The TWs previously isolated [13, 14] were induced us-

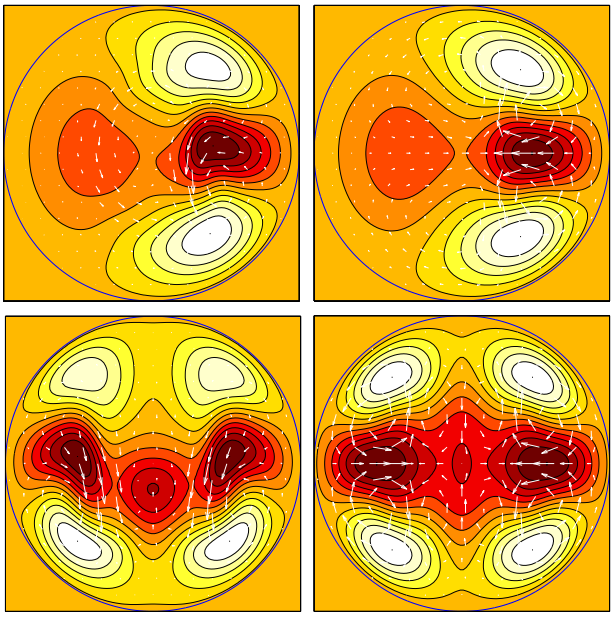

FIG. 1: Velocity fields for the asymmetric mode at $Re = 2900$ (top) and the mirror-symmetric mode at $Re = 1344$ (bottom) (both at $\alpha = 0.75$). An instantaneous state is shown on the left and a streamwise-averaged state on the right. The coloring indicates the downstream velocity relative to the parabolic laminar profile: red(dark) through white(light) represents slow through fast (with zero corresponding to the shading outside the pipe). In-plane velocity components are shown by vectors. The maximum and minimum streamwise velocities (with the laminar flow subtracted) and maximum in-plane speed for the asymmetric mode are 0.33, −0.42 and 0.03 respectively while for the mirror-symmetric mode they are 0.31, −0.43 and 0.08 (all in units of U).

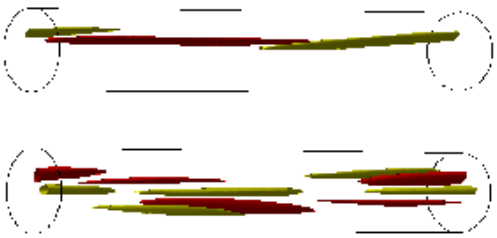

FIG. 2: Instantaneous axial vorticity along one wavelength of the pipe for the asymmetric mode (top) and the mirror-symmetric mode (bottom) at the same Re and α as Fig 1. Contours are at +/-60% of the maximum absolute value (green-light/red-dark).

ing a forcing that was rotationally symmetric under

$$\mathbf{R}_m : (u, v, w, p)(s, \phi, z) \to (u, v, w, p)(s, \phi + 2\pi/m, z)$$

for some $m = 2, 3, 4, 5$ or 6. As well as this rotational symmetry, all the TWs also possess the shift-&-reflect

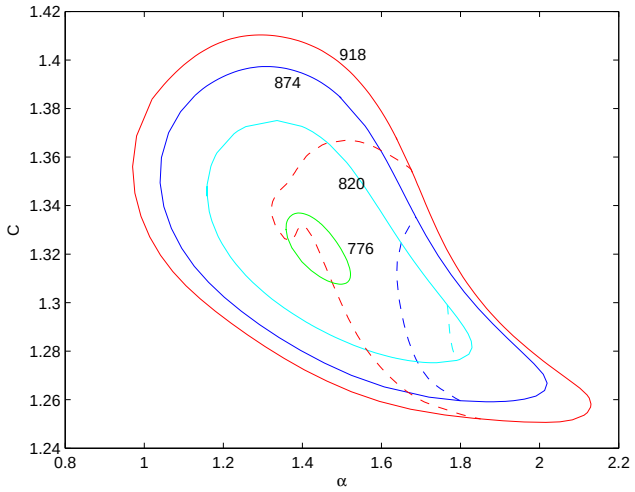

FIG. 3: Phase velocity C in units of U as a function of α for the mirror-symmetric modes (solid lines) and asymmetric modes (dashed) at 4 values of Re near the saddle node bifurcation at $Re = 773$.

symmetry

$$\mathbf{S} : (u, v, w, p)(s, \phi, z) \to (u, -v, w, p)(s, -\phi, z + \pi/\alpha)$$

where α is the base axial wavenumber (so the periodic pipe is $2\pi/\alpha$ long) and take the form $\boldsymbol{u}(s, \phi, z, t) = \boldsymbol{u}(s, \phi, z - Ct)$ where C is the *a priori* unknown axial phase speed of the wave. In contrast, new rotationally-asymmetric TWs were found by using a forcing function which created vortices with the radial velocity structure $u(s, \phi) \propto \Re e\{ e^{-1/s}(1 - s^2) \sum_{m=1}^{7} [1 + \cos(\frac{m\pi}{7})] e^{im\phi} \}$ and hence distributed energy across a band of azimuthal wavenumbers. This choice led to a branch of asymmetric solutions whose component fast and slow streaks are preferentially located to one side of the pipe (see Figs 1 and 2). These asymmetric TWs are **S**-symmetric and have one phase speed C along the pipe. They extend beyond $Re = 5000$ and originate at a pitchfork bifurcation (at $Re = 1770$ when $\alpha = 0.75$) from a mirror-symmetric TW family (see Figs 1 and 2) which satisfies the additional shift-&-rotate symmetry

$$\emptyset : (u, v, w, p)(s, \phi, z) \to (u, v, w, p)(s, \phi + \pi, z + \pi/\alpha)$$

(coupled with the **S**-symmetry, this implies invariance under reflection in the line $\phi = \pm\pi/2$). The mirror-symmetric solutions undergo a saddle node bifurcation at much lower Re: $Re = 1167$ at $\alpha = 0.75$ going down to a minimum of $Re = 773$ at $\alpha = 1.44$: see Fig. 3. The friction factors associated with the upper branches of these new modes are much larger than the rotationally-symmetric modes [13, 14] (see Fig. 4).

Both new families possess the characteristic features of the TWs found in [13, 14]: essentially 2-dimensional fast streaks near the wall and aligned with the flow, slow streaks in the interior which are aligned on average with

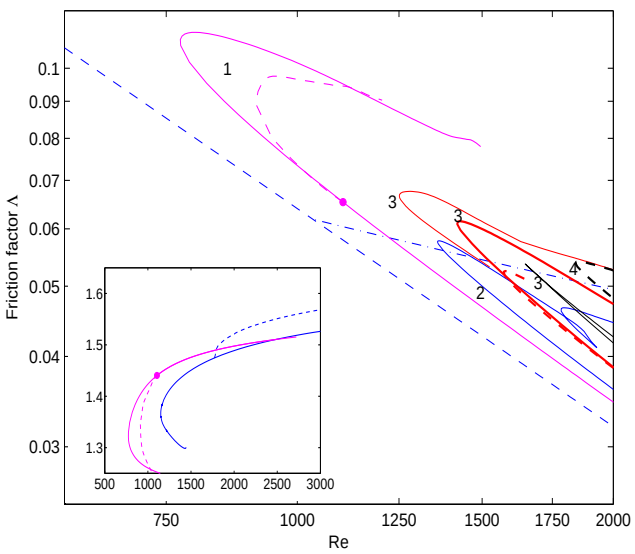

FIG. 4: Friction factor $\Lambda := 2D\,G/\rho U^2$ against Re for the various families of travelling waves where G is the mean pressure gradient along the pipe and ρ the density. The lower dashed line indicates the laminar value $\Lambda_{lam} = 64/Re$ and the upper dash-dot line indicates the log-law parametrization of experimental data $1/\sqrt{\Lambda} = 2.0\log(Re\sqrt{\Lambda})$. The labels are m values for the rotational symmetry $\mathbf{R}_m$ of the different TW families all drawn at the wavenumber which leads to the lowest saddle node bifurcation. The new TWs shown - mirror-symmetric modes (solid) and asymmetric modes (dashed) - correspond to $m = 1$ and $\alpha = 1.44$. The bifurcation point is marked with a dot. The inset shows the phase velocity C (in units of U) versus Re for the two types of mode at $\alpha = 0.75$ where the bifurcation was originally found and the optimum $\alpha = 1.44$.

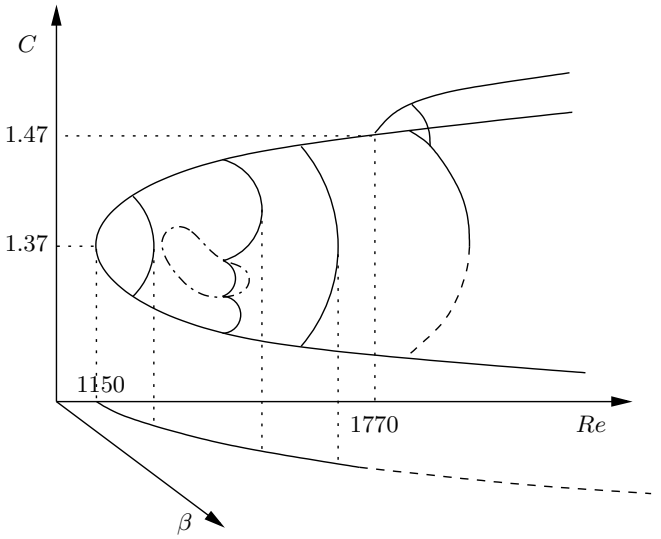

FIG. 5: A schematic picture of how all the new travelling wave branches fit together in (β, Re, C) space (at $\alpha = 0.75$). The main parabolic curve in the $\beta = 0$ plane is the mirror-symmetric branch off which the asymmetric branch bifurcates (uppermost line). Helical branches bulge out of the $\beta = 0$ plane and connect upper and lower parts of the mirror-symmetric. Across a finite range of Re, these helical modes perforate the $\beta = 0$ plane in between the mirror-symmetric branches creating an isola of non-helical rotating TWs (closed dash-dot loop). Helical waves also connect the asymmetric branch and the helical solutions which originate from the mirror-symmetric solutions.

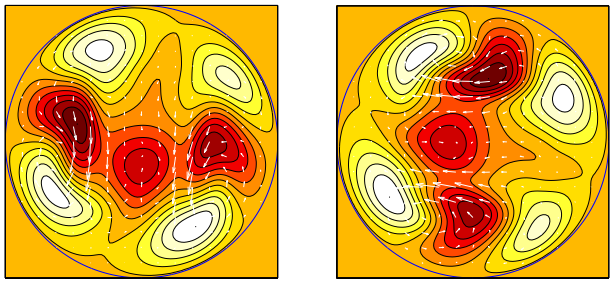

FIG. 6: Two velocity slices across a helical mode taken at the same instant of time but 25 D apart with $\alpha = 0.75$, $\beta = 0.019$, $\omega = -0.0011$ at $Re = 1344$. The velocity representation is as in Fig. 1.

the flow, and a smaller (typically by an order of magnitude) 3-dimensional wave field. By continuity, helical TWs should exist with these fast streaks inclined to the flow direction and indeed a surface of such solutions can be found connecting the upper and lower branches of the mirror-symmetric TWs (see Fig. 5). These helical TWs take the form $\boldsymbol{u}(s,\phi,z,t) = \boldsymbol{u}(s,\phi-\beta[z-Ct]-\omega t, z-Ct)$ with β measuring the helicity in the Galilean frame moving at $C\hat{\mathbf{z}}$ and ω being an azimuthal phase speed *relative* to the Galilean frame. Helicity destroys **S**-symmetry but a modified form of Ø-symmetry ($Ø_\beta$) is preserved where the rotation transformation is now $\phi \to \phi + (1 - \frac{\beta}{\alpha})\pi$. The helicity β and rotational speed ω never rise above $O(10^{-2})$ for $Re \leq 1500$ confirming the flow preference for non-rotating, axially-aligned streaks. Interestingly, in the range $Re = 1165 - 1330$, the helicity β on this surface passes through zero twice in going between the two mirror-symmetric branches (see Fig. 5). These points correspond to an isola in the (fixed α) C vs Re plane of rotating non-helical modes which are neither shift-&-reflect symmetric nor have any rotational symmetry. The helical and non-helical rotating waves look very similar to the mirror-symmetric modes except for a slight twist in the streak structure along the pipe (see Figs 6 and 7). Helical modes continued off the asymmetric modes have no symmetry at all and originate in a symmetry-breaking bifurcation off the $Ø_\beta$-symmetric helical solutions extended from the mirror-symmetric waves: see Fig. 5.

The asymmetric, mirror-symmetric and helical TWs all represent saddle points in phase space with a very low-dimensional unstable manifolds (e.g. 2 for the asymmetric mode at $(\alpha, Re) = (0.75, 1820)$ and 4 for the mirror-symmetric mode at $(\alpha, Re) = (0.75, 1184)$). Their presence indicates the richness of phase space even at

FIG. 7: The four fast streaks of the helical mode shown in Fig. 6 plotted over one β wavelength $\approx 170\,D$.

Reynolds numbers approaching 773. The delay of transition until $Re \geq 1750$ suggests that the establishment of a 'turbulence-bearing' scaffold constituted of all their stable and unstable manifolds is far from immediate. The clear implication is that while the emergence of alternative solutions to the laminar state seems a necessary precursor for transition, it is *not* a good predictor of the actual Reynolds number at which this occurs in pipe flow (and other shear flow systems). Once the transitional regime has been reached however, there is now mounting experimental [24, 25] and numerical evidence [26, 27] indicating that some of the travelling waves at least (those with low to intermediate wall shear stresses [26]) appear as transient but recurrent coherent structures within the flow. Intriguingly, numerical simulations [26] have also revealed that a number of travelling waves with low wall shear stress sit on a dividing surface in phase space (a separatrix if the turbulence is a sustained state) which separates initial conditions which directly relaminarise and those which lead to a turbulent episode. Recent computations [28, 29] using a shooting technique to converge onto this dividing surface appear to have already found that the asymmetric wave sits there too (compare Fig 1 to Fig. 8 of [29] and Fig. 1 of [28]). The fact that this wave bears some resemblence to $m = 1$ 'optimal' disturbances which emerge from linear transient growth analyses also suggests an enticing opportunity to bridge the gap between linear and nonlinear approaches.

In summary, we have presented a series of new travelling wave solutions to the pipe flow problem which have different structure to existing solutions and which exist at far lower Reynolds numbers. One type - the asymmetric modes - represents the missing $m = 1$ family from the waves found initially [13, 14]. These waves also appear to rationalise some interesting results from recent numerical computations [28, 29], thereby corroborating the picture which is emerging that lower branch TWs (and therefore also their stable manifolds) sit on the separatrix between laminar and turbulent states.

We acknowledge encouraging discussions with Fabian Waleffe and the support of EPSRC.

* Electronic address: Chris.Pringle@bris.ac.uk
† Electronic address: R.R.Kerswell@bris.ac.uk

[1] O. Reynolds, Proc. R. Soc. Lond. **35**, 84 (1883).
[2] G. H. L. Hagen, Poggendorfs Annalen der Physik und Chemie **16**, 423 (1839).
[3] J. L. M. Poiseuille, Comptes Rendus de l'Académie des Sciences **11**, 961,1041 (1840).
[4] A. M. Binnie and J. S. Fowler, Proc. Roy. Soc. Lond. **A 192**, 32 (1947).
[5] E. R. Lingren, Arkiv für Physik **12**, 1 (1958).
[6] R. J. Leite, J. Fluid Mech. **5**, 81 (1959).
[7] I. J. Wygnanski and F. H. Champagne, J. Fluid Mech. **59**, 281 (1973).
[8] A. G. Darbyshire and T. Mullin, J. Fluid Mech. **289**, 83 (1995).
[9] B. Hof, A. Juel, and T. Mullin, Phys. Rev. Lett. **91**, 244502 (2003).
[10] J. Peixinho and T. Mullin, Proc. IUTAM Symp. on Laminar-Turbulent Transition (eds Govindarajan, R. and Narasimha, R.) pp. 45–55 (2005).
[11] J. Peixinho and T. Mullin, Phys. Rev. Lett. **96**, 094501 (2006).
[12] A. P. Willis and R. R. Kerswell, Phys. Rev. Lett. **98**, 014501 (2007).
[13] H. Faisst and B. Eckhardt, Phys. Rev. Lett. **91**, 224502 (2003).
[14] H. Wedin and R. R. Kerswell, J. Fluid Mech. **508**, 333 (2004).
[15] P. J. Schmid and D. S. Henningson, J. Fluid Mech. **277**, 197 (1994).
[16] S. Bottin, O. Dauchot, F. Daviaud, and P. Manneville, Phys. Fluids **10**, 2597 (1998).
[17] M. Nagata, J. Fluid Mech. **217**, 519 (1990).
[18] F. Waleffe, Phys. Fluids **15**, 1517 (2003).
[19] S. J. Davies and C. M. White, Proc. Roy. Soc. **A 119**, 92 (1928).
[20] T. W. Kao and C. Park, J. Fluid Mech. **43**, 145 (1970).
[21] V. C. Patel and M. R. Head, J. Fluid Mech. **38**, 181 (1969).
[22] S. A. Orszag and L. C. Kells, J. Fluid Mech. **96**, 159 (1980).
[23] D. R. Carlson, S. E. Widnall, and M. F. Peeters, J. Fluid Mech. **121**, 487 (1982).
[24] B. Hof and et al, Science **305**, 1594 (2004).
[25] B. Hof, C. W. H. van Doorne, J. Westerweel, and F. T. M. Nieuwstadt, Phys. Rev. Lett. **95**, 214502 (2005).
[26] R. R. Kerswell and O. R. Tutty, J. Fluid Mech. in press (arXiv.org/physics/0611009) (2007).
[27] T. M. Schneider, B. Eckhardt, and J. Vollmer, Preprint (arXiv.org/physics/0611020) (2007).
[28] T. M. Schneider and B. Eckhardt, Chaos **16**, 041103 (2006).
[29] B. Eckhardt, T. M. Schneider, B. Hof, and J. Westerweel, Annual Review of Fluid Mechanics **39**, 447 (2007).
[30] In the nomenclature of [14], typical resolutions used to represent the modes were $(15, 25, 5)$ representing about 20,000 degrees of freedom.